IEEE Access
Multidisciplinary | Rapid Review | Open Access Journal

SPECIAL SECTION ON MISSION CRITICAL SENSORS AND SENSOR NETWORKS (MC-SSN)

Received December 10, 2018, accepted January 6, 2019, date of publication January 21, 2019, date of current version February 20, 2019.

Digital Object Identifier 10.1109/ACCESS.2019.2893452

Off-Grid DOA Estimation for Wideband LFM Signals in FRFT Domain Using the Sensor Arrays

XIUHONG WANG[1], BO LI[1], HONGJUAN YANG[1], AND WEIDANG LU[2], (Member, IEEE)
[1]School of Information Science and Engineering, Harbin Institute of Technology at Weihai, Weihai 264209, China
[2]College of Information Engineering, Zhejiang University of Technology, Hangzhou 310014, China

Corresponding author: Hongjuan Yang (hjyang@hit.edu.cn)

This work was supported in part by the Natural Science Foundation of Shandong Province under Grant ZR2018PF001 and Grant ZR2014FP016, in part by the National Natural Science Foundation of China under Grant 61871348 and Grant 61571157, and in part by the Fundamental Research Funds for the Central Universities under Grant HIT. NSRIF. 201720 and Grant HIT. NSRIF. 2016100.

ABSTRACT For the direction-of-arrival (DOA) estimators based on sparse signal representation, the feasibility and precision are greatly restricted by the inherent limitation of the predefined spatial discrete grids. In this paper, based on the high aggregation characteristic of wideband linear frequency modulation signals, we derive the modified fractional domain sparse model (MFDSM) in DOA estimation and propose a novel off-grid DOA estimation method via alternating descent iteration (OGDEADI). The simulation results show that our proposed MFDSM-OGDEADI method has enhanced estimation accuracy and better angular resolution in terms of signal-to-noise ratio, angle difference, grid size, and angle bias, and it also has the advantage of being less sensitive to the grid size.

INDEX TERMS Direction-of-arrival estimation, sensor arrays, off-grid targets, sparse signal representation, wideband signals.

I. INTRODUCTION

In recent years, research and applications related to sensors and sensor networks (SSN) have received more and more attention, which have been applied to a lot of missions such as battlefield, search and rescue, surveillance, and so on. Using sensor arrays in Direction-of-arrival (DOA) estimation has also been a hot research topic in the past decades, which is widely applied to radar, sonar, communications, seismic exploration and other fields [1]–[3]. The algorithms proposed to solve this problem are generally designed for the narrowband stationary signals. However, with the development of signal processing technology, wideband signal DOA estimation has also drawn more and more attention [4]–[7].

The most classical DOA estimation methods of wideband signal are incoherent signal subspace method (ISSM) [8] and coherent signal subspace method (CSSM) [9]. With a filter bank or the discrete Fourier transform (DFT), the two methods decompose wideband signals into many narrowband signals and then they use narrowband signal DOA estimation methods to estimate wideband signals. The ISSM methods cannot estimate the coherent wideband signals and have relatively low precision. The CSSM methods provide outstanding estimation accuracy and relatively low computational complexity, but their prerequisite is that a lot of snapshots are needed. Furthermore, most of these algorithms need the focusing matrices which require pre-estimating the DOA angles. However, these focusing matrices are sensitive to the DOA values which are pre-estimated, especially when the estimated error is large, the estimation performance of the algorithm is degraded.

Recently, sparse signal representation (SSR), an emerging area in signal processing, has been introduced to DOA estimation [10]–[13] where the conventional DOA estimation will be transformed into an SSR problem by the sparsity-inducing techniques [14], [15]. The SSR based estimators exhibit superior performance compared to spectrum-based ones, especially when signal-to-noise-ratio (SNR) is low, snapshots are limited and signals are coherent, their disadvantages should not be ignored. The sparsity based DOA estimators explore the incident signals' spatial sparsity, i.e., the angle space is divided into a large number of grids where the source directions of interest are assumed to exactly lie on some of the grids. However, a too coarse or too dense grid set may bring unpleasant results. In particular, a coarse grid set cannot achieve satisfactory estimation accuracy. On the

The associate editor coordinating the review of this manuscript and approving it for publication was Qilian Liang.

other hand, a compact grid set may lead to the high modeling error and the high computation complexity [16]. Hence, some researchers [17]–[20] have focused on the off-grid case, where the unknown DOAs are not limited onto the grids.

To our best knowledge, the off-grid case was originally studied in [21]. For perturbed compressive sensing under sparsity constraints, the authors proposed a sparsity-cognizant total least-squares (S-TLS) method. However, this paper mainly focuses on generalized algorithms rather than on DOA estimation. In [22], a new algorithm based on sparse Bayesian inference (SBI) is applied for the off-grid case to achieve a high DOA resolution from a coarse sampling grid. Firstly, a first-order Taylor expansion-based model is established. Then, a new algorithm named OGSBI is proposed to solve this model from a Bayesian inference perspective where the sparse prior is exploited by assuming a Laplace prior for the signal of interest. Additionally, an iterative alternating descent algorithm was developed in [23] based on first order Taylor expansion, which can simultaneously make DOA angle estimation and deal with the off-grid problem. In general, these algorithms are for narrowband signals, and for wideband signals, there is not much research literature.

Linear frequency modulation (LFM) signals have been extensively applied in radar, sonar, seismic detection and so on. However it is a non-stationary signal and cannot be handled by the traditional DOA estimation algorithms with high resolution. Therefore time-frequency analysis tools are introduced to solve this problem. As a powerful time-frequency analysis tool, Fractional Fourier transform (FRFT) [24]–[26] can reflect the signal characteristic in time domain and frequency domain simultaneously. FRFT has many significant advantages, such as excellent aggregation characteristics to LFM signals, and no cross-term interference. Also in FRFT, there are no frequency point selection problems of the secondary time-frequency distribution [27]–[29], and LFM signals can be separated while the parameters also can be estimated easily. Therefore, through the integration of array signal processing technology and FRFT transform, it is easier to achieve wideband LFM signals' DOA estimation and provides better estimation effect compared with other time-frequency analysis methods. In this paper, we focus on wideband LFM signal DOA estimation problems under grid mismatch conditions. The modified fractional domain sparse model (MFDSM) is introduced and a novel off-grid DOA estimation method via alternating descent iteration (OGDEADI) is proposed based on MFDSM model.

The rest of the paper is organized as follows: in Section II, DOA estimation models of wideband LFM signals in the time domain and FRFT domain are introduced. Then, FRFT domain based off-grid DOA model is introduced in Section III. In Section IV, an off-grid DOA estimation algorithm based on alternating descending iteration is proposed. Subsequently, the simulation results and analysis are stated in Section V. Finally, we summarize the paper in Section VI.

II. WIDEBAND LFM SIGNAL DOA ESTIMATION MODEL

A. TIME DOMAIN MODEL

Suppose there are K far-field wideband signals, $s_k(t), k = 1, 2, \cdots, K$, which are incident on a receiving array, and their angle of incidence are $(\theta_1, \theta_2, \cdots, \theta_K)$ respectively. We take a uniform linear array (ULA) with the array spacing d, and the number of array sensors is M as the receiving array.

Denote the kth LFM signal as

$$s_k(t) = C_k \exp\left[j\pi\left(2f_k t + \mu_k t^2\right)\right], \quad |t| \le \frac{T}{2} \tag{1}$$

where C_k is the amplitude, f_k is the center frequency, μ_k is the frequency slope and T is the pulse width of the kth LFM signal, respectively.

The mth array sensor's received signal can be represented as

$$r_m(t) = \sum_{k=1}^{K} s_k(t - \tau_{mk}) + n_m(t) \tag{2}$$

where $n_m(t)$ is the received noise signal, τ_{mk} represents the relative delay between the received signal by the mth sensor and the reference signal received by the first sensor, and for ULA, it can be expressed as $\tau_{mk} = (m-1)\, d \sin(\theta_k)/c$, in which c is the speed of light. By substituting the LFM signal expression into (2), the received signal can be further expressed as

$$r_m \triangleq (t) \sum_{k=1}^{K} a_m(\theta_k, t)\, s_k(t) + n_m(t) \tag{3}$$

In (3), $a_m(\theta_k, t)$ is the array steering vector on the mth array sensor, and expressed as

$$a_m(\theta_k, t) = \exp\left[-j2\pi\left(f_k + \mu_k t\right)\tau_{mk} + j\pi\mu_k\tau_{mk}^2\right], \quad \text{for } m = 1, 2, \cdots, M \tag{4}$$

By integrating all the signals received by the array together, (3) can be written as

$$\boldsymbol{r}(t) = \boldsymbol{A}(\theta, t)\,\boldsymbol{s}(t) + \boldsymbol{n}(t) \tag{5}$$

where $\boldsymbol{r}(t) = [r_1(t), \cdots, r_M(t)]^T$ and $\boldsymbol{n}(t) = [n_1(t), \cdots, n_M(t)]^T$ represent the received signal and the noise vector, $\boldsymbol{s}(t) = [s_1(t), \cdots, s_K(t)]^T$ represents the incident source signal vector. $\boldsymbol{A}(\theta, t) = [\boldsymbol{a}(\theta_1, t), \cdots, \boldsymbol{a}(\theta_K, t)]_{M\times K}$ is the array manifold matrix in which $\boldsymbol{a}(\theta_k, t)$ is the steering vector of the kth wideband LFM signal expressed as

$$\begin{aligned}\boldsymbol{a}(\theta_k, t) &= \begin{bmatrix} a_1(\theta_k, t) \\ a_2(\theta_k, t) \\ \vdots \\ a_M(\theta_k, t) \end{bmatrix} \\ &= \begin{bmatrix} \exp\left\{-j2\pi\left(f_k + \mu_k t\right)\tau_{1k} + j\pi\mu_k\tau_{1k}^2\right\} \\ \exp\left\{-j2\pi\left(f_k + \mu_k t\right)\tau_{2k} + j\pi\mu_k\tau_{2k}^2\right\} \\ \vdots \\ \exp\left\{-j2\pi\left(f_k + \mu_k t\right)\tau_{Mk} + j\pi\mu_k\tau_{Mk}^2\right\} \end{bmatrix} \\ &\quad \text{for } k = 1, 2, \cdots, K \end{aligned} \tag{6}$$

As can be seen in (6), the array steering vector varies along with time $\boldsymbol{t}$ and this fact would result in that the traditional DOA estimation methods cannot be applied to the wideband LFM signal DOA estimation, since these traditional methods are with the assumption that the array steering vector is time-invariant and stationary.

B. FRFT DOMAIN MODEL

As an effective time-frequency analysis tool, FRFT transform has an aggregation effect on LFM signals and can take the LFM signal's energy together [24]. Using this feature, we consider introducing FRFT transform into the data processing.

Firstly, the FRFT transform is performed on the received signal of the mth sensor

$$R_m(u,\alpha) = \mathscr{F}^p[r_m(t)] \triangleq \sum_{k=1}^{K} Z_m^k(u,\alpha) + N_m(u,\alpha) \quad (7)$$

where $Z_m^k(u,\alpha)$ and $N_m(u,\alpha)$ are the FRFT transform of the signal $s_k(t-\tau_{mk})$ and the noise $n_m(t)$, respectively. The transformed variable u is called the FRFT domain, and can also be called fractional domain (FD) [25].

In view of FRFT transform's time-shifting characteristics [24], $Z_m^k(u,\alpha)$ in (7) can be expressed as

$$\begin{aligned} Z_m^k(u,\alpha) &= S^k(u-\tau_{mk}\cos\alpha,\alpha) \\ &\quad\cdot \exp\left(j\pi\tau_{mk}^2\sin\alpha\cos\alpha - j2\pi u\tau_{mk}\sin\alpha\right) \end{aligned} \quad (8)$$

In (8), $S^k(u,\alpha)$ is the signal $s_k(t)$'s FRFT transform, and then

$$\begin{aligned} S^k(u,\alpha) &= \sqrt{\frac{1-j\cot\alpha}{2\pi}}\exp\left(j\pi u^2\cot\alpha\right) \\ &\quad\cdot\int_{-T/2}^{T/2}\exp\left[j\pi t^2(\cot\alpha+\mu_k)\right. \\ &\quad\left. - j2\pi t(u\csc\alpha - f_k)\right]dt \end{aligned} \quad (9)$$

Substituting (9) into (8),

$$\begin{aligned} &Z_m^k(u,\alpha) \\ &= \sqrt{\frac{1-j\cot\alpha}{2\pi}}\cdot\exp\left(j\pi\tau_{mk}^2\sin\alpha\cos\alpha - j2\pi u\tau_{mk}\sin\alpha\right) \\ &\quad\cdot\exp\left(j\pi(u-\tau_{mk}\cos\alpha)^2\cot\alpha\right) \\ &\quad\cdot\int_{-T/2}^{T/2}\exp\left[j\pi t^2(\cot\alpha+\mu_k)\right. \\ &\quad\left. - j2\pi t((u-\tau_{mk}\cos\alpha)\csc\alpha - f_k)\right]dt \end{aligned} \quad (10)$$

From (10), we can see that, when $\alpha = -\text{arc}\cot(\mu_k) \triangleq \hat{\alpha}_k$, the clustering property of $Z_m^k(u,\alpha)$ is the best, thus Eq. (10) can be further reduced to

$$\begin{aligned} &Z_m^k(u,\hat{\alpha}_k) \\ &= \sqrt{\frac{1-j\cot\hat{\alpha}_k}{2\pi}} \\ &\quad\cdot T\frac{\sin\left[\pi\left((u-\tau_{mk}\cos\hat{\alpha}_k)\csc\hat{\alpha}_k - f_0\right)T\right]}{\left[\pi\left((u-\tau_{mk}\cos\hat{\alpha}_k)\csc\hat{\alpha}_k - f_0\right)T\right]} \\ &\quad\cdot\exp\left(j\pi\left(u-\tau_{mk}\cos\hat{\alpha}_k\right)^2\cot\hat{\alpha}_k\right) \\ &\quad\cdot\exp\left(j\pi\tau_{mk}^2\sin\hat{\alpha}_k\cos\hat{\alpha}_k - j2\pi u\tau_{mk}\sin\hat{\alpha}_k\right) \end{aligned} \quad (11)$$

As can be seen from the above, $Z_m^k(u,\hat{\alpha}_k)$ is a 1-D function of the variable u. When $\hat{u}_k = \tau_{mk}\cos\hat{\alpha}_k + f_0/\csc\hat{\alpha}_k$, the maximum value of $Z_m^k(u,\hat{\alpha}_k)$ can be obtained as

$$\begin{aligned} &Z_m^k(\hat{u}_k,\hat{\alpha}_k) \\ &= T\sqrt{\frac{1-j\cot\hat{\alpha}_k}{2\pi}}\cdot\exp\left(j\pi\left(f_0/\csc\hat{\alpha}_k\right)^2\cot\hat{\alpha}_k\right) \\ &\quad\cdot\exp\left(j\pi\tau_{mk}^2\sin\hat{\alpha}_k\cos\hat{\alpha}_k - j2\pi\hat{u}_k\tau_{mk}\sin\hat{\alpha}_k\right) \end{aligned} \quad (12)$$

When $m = 1$, that is, for the reference sensor, the delay $\tau = 0$, so (12) can be reduced as

$$Z_1^k(u,\alpha) = \mathscr{F}^p[s_k(t)] = S^k(u,\alpha) \quad (13)$$

Thus $Z_1^k(u,\alpha)$'s peak value is

$$\begin{aligned} Z_1^k(\hat{u}_{1,k},\hat{\alpha}_{1,k}) &= S^k(\hat{u}_{1,k},\hat{\alpha}_{1,k}) \\ &= T\sqrt{\frac{1-j\cot\hat{\alpha}_{1,k}}{2\pi}}\exp\left(j\pi\hat{u}_{1,k}^2\cot\hat{\alpha}_{1,k}\right) \end{aligned} \quad (14)$$

and the peak position coordinate is $(\hat{\alpha}_{1,k},\hat{u}_{1,k})$, which can be expressed as

$$\begin{cases} \hat{\alpha}_{1,k} = -\text{arc}\cot(\mu_k) \\ \hat{u}_{1,k} = f_0/\csc\hat{\alpha}_k \end{cases} \quad (15)$$

In view of (14), (12) can be further simplified as

$$\begin{aligned} Z_m^k(\hat{u}_k,\hat{\alpha}_k) &= S^k(\hat{u}_{1,k},\hat{\alpha}_{1,k})\cdot\exp\left(-j2\pi\hat{u}_{1,k}\tau_{mk}\sin\hat{\alpha}_{1,k}\right) \\ &\quad\cdot\exp\left(j\pi\tau_{mk}^2\sin\hat{\alpha}_{1,k}\cos\hat{\alpha}_{1,k}\right) \end{aligned} \quad (16)$$

In (16), the item of $\exp\left(j\pi\tau_{mk}^2\sin\hat{\alpha}_{1,k}\cos\hat{\alpha}_{1,k}\right)$ can be ignored thanks to τ_{mk}^2 is so small. As a result, we can obtain (16)'s further simplification

$$Z_m^k(\hat{u}_k,\hat{\alpha}_k) = S^k(\hat{u}_{1,k},\hat{\alpha}_{1,k})\cdot\exp\left(-j2\pi\hat{u}_{1,k}\tau_{mk}\sin\hat{\alpha}_{1,k}\right) \quad (17)$$

Then we can substitute (17) into (7) and obtain

$$\begin{aligned} &R_m(\hat{u}_k,\hat{\alpha}_k) \\ &= \sum_{k=1}^{K} S^k(\hat{u}_{1,k},\hat{\alpha}_{1,k})\cdot\exp\left(-j2\pi\hat{u}_{1,k}\tau_{mk}\sin\hat{\alpha}_{1,k}\right) \\ &\quad + N_m(\hat{u}_k,\hat{\alpha}_k) \end{aligned} \quad (18)$$

where $R_m\left(\hat{u}_k, \hat{\alpha}_k\right)$ is a certain peak value of the received signal's FRFT transform the mth sensor. By integrating all sensors' received signals together, (18) can be expressed with a matrix form as

$$\boldsymbol{R}\left(\hat{u}_k, \hat{\alpha}_k\right) = \boldsymbol{B}(\theta)\,\boldsymbol{S}\left(\hat{u}_{1,k}, \hat{\alpha}_{1,k}\right) + \boldsymbol{N}\left(\hat{u}_k, \hat{\alpha}_k\right) \tag{19}$$

where $\boldsymbol{R}\left(\hat{u}_k, \hat{\alpha}_k\right)$ is the corresponding peak-value vector of the received signal and $\boldsymbol{N}\left(\hat{u}_k, \hat{\alpha}_k\right)$ is the noise vector after FRFT transform. $\boldsymbol{B}(\theta) = [\boldsymbol{b}(\theta_1), \cdots, \boldsymbol{b}(\theta_K)]$ is the array manifold matrix, and in which $\boldsymbol{b}(\theta_k)$ is the kth LFM signal's steering vector with the expression

$$\boldsymbol{b}(\theta_k) = \begin{bmatrix} \exp\left(-j2\pi\,\tau_{1k}\hat{u}_{1,k}\sin\hat{\alpha}_{1,k}\right) \\ \exp\left(-j2\pi\,\tau_{2k}\hat{u}_{1,k}\sin\hat{\alpha}_{1,k}\right) \\ \vdots \\ \exp\left(-j2\pi\,\tau_{Mk}\hat{u}_{1,k}\sin\hat{\alpha}_{1,k}\right) \end{bmatrix} \tag{20}$$

where for the ULA arrays, $\tau_{mk} = (m-1)\,d\sin(\theta_k)/c$.

In view of (20), unlike (6) in time domain, the steering vector in FRFT domain does not vary along with time $\boldsymbol{t}$. As a result, we can apply the traditional narrowband DOA estimation methods to the DOA estimation model obtained from (19) in the FRFT domain. In other words, applying FRFT transform to the wideband LFM signals will make the DOA estimation model of wideband LFM signals transform into a similar estimation model of narrowband signals.

III. OFF-GRID DOA MODEL BASED ON FRFT DOMAIN

A. SPARSE DOA MODEL BASED ON FRFT DOMAIN

Combined with the above analysis, a sparse representation model based on FRFT domain (FDSM) of DOA estimation will be obtained by deriving the DOA estimation model in FRFT domain from (19).

Firstly, divide the whole angle space evenly into L parts ($L \gg K$), so that we can obtained the discretized sampling grid set $\boldsymbol{\Theta} \triangleq \left\{\bar{\theta}_1, \bar{\theta}_2, \cdots, \bar{\theta}_L\right\}$. In view of (20), a redundant dictionary can be generated as (21), which consists of an over-complete steering vector set corresponding to the angle $\boldsymbol{\Theta}$.

$$\boldsymbol{\Psi}(\boldsymbol{\Theta}) = \left\{\boldsymbol{b}\left(\bar{\theta}_1\right), \boldsymbol{b}\left(\bar{\theta}_2\right), \cdots, \boldsymbol{b}\left(\bar{\theta}_L\right)\right\} \tag{21}$$

For convenience, we can define the sparse vector $\boldsymbol{H} \triangleq \{h_1, h_2, \cdots, h_L\}$ as the signal amplitude values corresponding to all potential directions $\boldsymbol{\Theta}$. The element h_i is not zero when there is a signal from the angle $\bar{\theta}_i$, and its value is equal to the corresponding peak value after the FRFT transform. The element h_i is equal to 0 when there is no signal from the potential incident direction, that is

$$h_i = \begin{cases} S^k\left(\hat{u}_{1,k}, \hat{\alpha}_{1,k}\right), & \bar{\theta}_i \in \{\theta_1, \theta_2, \cdots, \theta_K\} \\ 0, & \bar{\theta}_i \notin \{\theta_1, \theta_2, \cdots, \theta_K\} \end{cases} \tag{22}$$

Therefore, the sparse representation model based on FRFT domain of DOA estimation can be obtained as

$$\boldsymbol{R} = \boldsymbol{\Psi}(\boldsymbol{\Theta})\,\boldsymbol{H} + \boldsymbol{N} \tag{23}$$

where $\boldsymbol{R}$ and $\boldsymbol{N}$ are the received signal peak-value vector and the noise vector after the FRFT transform on all the sensors.

B. OFFGRID DOA MODEL BASED ON FRFT DOMAIN

Consider the true DOA angles cannot be right the elements in set $\boldsymbol{\Theta}$. An off-grid model is proposed in [21]. Suppose for some DOAs, they are not right on the discretized sampling grid, i.e., $\theta_k \notin \left\{\bar{\theta}_1, \bar{\theta}_2, \cdots, \bar{\theta}_L\right\}$ for some $k \in \{1, 2, \cdots, K\}$. Note the nearest grid point to θ_k as $\bar{\theta}_{l_k}$, $l_k \in \{1, 2, \cdots, L\}$. Therefore the first-order linear approximation for the steering vector $\boldsymbol{b}(\theta_k)$ can be written as

$$\boldsymbol{b}(\theta_k) = \boldsymbol{b}\left(\bar{\theta}_{l_k}\right) + \boldsymbol{d}\left(\bar{\theta}_{l_k}\right)\left(\theta_k - \bar{\theta}_{l_k}\right) \tag{24}$$

where $\boldsymbol{d}\left(\bar{\theta}_{l_k}\right) = \boldsymbol{b}'\left(\bar{\theta}_{l_k}\right)$.

According to the formula (20),

$$\boldsymbol{d}\left(\bar{\theta}_{l_k}\right) = \left(j2\pi\,\hat{u}_k\sin\hat{\alpha}_k\boldsymbol{p}\sin\left(\bar{\theta}_{l_k}\right)/c\right) \odot \boldsymbol{b}\left(\bar{\theta}_{l_k}\right) \tag{25}$$

where "$\odot$" denotes the element wise Hadamard product. $\boldsymbol{p} = [0, d, 2d, \cdots, (M-1)\,d]^T$, d is the sensor spacing.

For convenience, define a redundant derivative matrix $\boldsymbol{D}$ and its each column is the derivative $\boldsymbol{d}\left(\bar{\theta}_i\right)$ of the grid angle $\bar{\theta}_i$, i.e., $\boldsymbol{D} = \left\{\boldsymbol{d}\left(\bar{\theta}_1\right), \cdots, \boldsymbol{d}\left(\bar{\theta}_L\right)\right\}$. $\theta_k - \bar{\theta}_{l_k}$ is the deviation of the true DOA and the most closed grid, expressed as Δ. Define a deviation vector $\boldsymbol{\Gamma} = [\Delta_1, \cdots, \Delta_L]^{\mathrm{T}}$ to satisfy

$$\begin{cases} \Delta_l = \theta_k - \bar{\theta}_{l_k}, & \text{if } l = l_k, k \in \{1, \ldots, K\} \\ \Delta_l = 0, & \text{others} \end{cases} \tag{26}$$

Therefore, under the grid mismatch conditions the off-grid DOA estimation model can be formulated as

$$\boldsymbol{R} = [\boldsymbol{\Psi} + \boldsymbol{D}\boldsymbol{\Pi}]\,\boldsymbol{H} + \boldsymbol{N} \tag{27}$$

where $\boldsymbol{R} = \left[R_0\left(\hat{u}, \hat{\alpha}\right), \cdots, R_{M-1}\left(\hat{u}, \hat{\alpha}\right)\right]^T$ and $\boldsymbol{N} = \left[N_0\left(\hat{u}, \hat{\alpha}\right), \cdots, N_{M-1}\left(\hat{u}, \hat{\alpha}\right)\right]^T$ are the single snapshot data vectors and the noise vectors consisting of the peaks after FRFT-transform of received signals and noise on all array sensors, respectively. $\boldsymbol{\Pi} = \mathrm{diag}(\boldsymbol{\Gamma})$ is a diagonal matrix consisting of angular deviations.

IV. OFF-GRID DOA ESTIMATION ALGORITHM BASED ON ALTERNATING DESCENDING ITERATION

For the modified fractional domain sparse model (MFDSM) of (27), under the condition that both the variable $\boldsymbol{H}$ and $\boldsymbol{\Gamma}$ are unknown, the optimal solution can be solved by the following problems

$$\min_{\boldsymbol{H},\boldsymbol{\Gamma}} \|\boldsymbol{R} - [\boldsymbol{\Psi} + \boldsymbol{D}\boldsymbol{\Pi}]\,\boldsymbol{H}\|_2^2 + \lambda\,\|\boldsymbol{H}\|_1 + \|\boldsymbol{\Gamma}\|_2^2 \tag{28}$$

The problem of (28) is a non-convex problem, thus it cannot be solved by the methods of convex optimization, moreover, the optimization problem contains two unknown variable vectors, therefore it is so difficult to solve directly.

Here we seek a sub-optimal method, which uses the idea of alternating descending iteration. In the optimization a variable is fixed, which the original optimization problem would be transformed into the sub problem of another variable, thus the non-convex problem is also relaxed into a convex problem. The convex problem is solved, and then the final solution is obtained by alternating descending iterations.

TABLE 1. MFDSM-OGDEADI algotithm steps.

Input: the received signal $\boldsymbol{r}$

Model establishment: Performing FRFT transform on the received signal $\boldsymbol{r}$ to obtain the single snapshot data $\boldsymbol{R}$ from the peaks in fractional domain, and the redundancy matrix $\boldsymbol{\Psi}$ and its derivative matrix $\boldsymbol{D}$ are constructed.

Initialization: $\boldsymbol{\Gamma}^{(0)} = \mathbf{0}_{L\times 1}$, the number of iterations is $n = 1$;

Iteration process:

（1）update $\boldsymbol{H}^{(n)}$: Solving problems with ReFOCUSS[31] algorithm $\min_{\boldsymbol{H}} \left\| \boldsymbol{R} - \left[\boldsymbol{\Psi} + \boldsymbol{D}\boldsymbol{\Pi}^{(n)} \right] \boldsymbol{H} \right\|_2^2 + \lambda \|\boldsymbol{H}\|_1$, where $\boldsymbol{\Pi}^{(n)} = \mathrm{diag}\left(\boldsymbol{\Gamma}^{(n)}\right)$;

（2）update $\boldsymbol{\Gamma}^{(n)} = \left(\boldsymbol{D}\bar{\boldsymbol{H}}^{(n)}\right)^{\dagger} \boldsymbol{E}^{(n)}$, where residual signal $\boldsymbol{E}^{(n)} = \boldsymbol{R} - \boldsymbol{\Psi}\boldsymbol{H}^{(n)}$;

（3）Determine whether $\left\| \boldsymbol{\Gamma}^{(n)} - \boldsymbol{\Gamma}^{(n-1)} \right\| \le \varepsilon$ or n exceeds the maximum iteration number, if satisfied, the iteration ends, otherwise continue $n = n + 1$;

Output: Sparse solution is $\hat{\boldsymbol{H}} = \boldsymbol{H}^{(n)}$, angle deviation is $\hat{\boldsymbol{\Gamma}} = \boldsymbol{\Gamma}^{(n)}$.

To do this, firstly we can look for a solution to the regularized least squares by keeping the unknown vector $\boldsymbol{\Gamma}$ fixed and solve for $\boldsymbol{H}$. Therefore, at the kth iteration of the algorithm we need to solve the sparse recovery problem:

$$\min_{\boldsymbol{H}} \left\| \boldsymbol{R} - \left[\boldsymbol{\Psi} + \boldsymbol{D}\boldsymbol{\Pi}^{(n)} \right] \boldsymbol{H} \right\|_2^2 + \lambda \|\boldsymbol{H}\|_1 \tag{29}$$

The sparse problem (29) can be solved by l_1-norm minimization or alternatively by greedy approaches such as SOMP.

Once $\boldsymbol{H}$ has been updated, we minimize over $\boldsymbol{\Gamma}$ keeping the current estimate of $\boldsymbol{H}$ fixed. In this case, the problem of (28) reduces to:

$$\min_{\boldsymbol{\Gamma}} \|\boldsymbol{R} - [\boldsymbol{\Psi} + \boldsymbol{D}\boldsymbol{\Pi}]\boldsymbol{H}\|_2^2 + \|\boldsymbol{\Gamma}\|_2^2 \tag{30}$$

The optimal solution of the problem (30) can be solved by deriving the cost function equal to zero. At the same time, the problem (30) can be proven to have a closed form solution and is equivalent to the following Least Square (LS) problem [30]:

$$\boldsymbol{R} - \boldsymbol{\Psi}\boldsymbol{H} = \boldsymbol{D}\boldsymbol{\Pi}\boldsymbol{H} \tag{31}$$

According to the property of the diagonal matrix, there is $\boldsymbol{D}\boldsymbol{\Pi}\boldsymbol{H} = \boldsymbol{D}\bar{\boldsymbol{H}}\boldsymbol{\Gamma}$, where $\bar{\boldsymbol{H}} \triangleq diag\,(h_1, h_2, \cdots, h_L)$. Therefore, (31) can be further reduced to

$$\boldsymbol{R} - \boldsymbol{\Psi}\boldsymbol{H} = \boldsymbol{D}\bar{\boldsymbol{H}}\boldsymbol{\Gamma} \tag{32}$$

Therefore, the least squares solution of a variable $\boldsymbol{\Gamma}$ can be expressed as

$$\boldsymbol{\Gamma}^* = \left(\boldsymbol{D}\bar{\boldsymbol{H}}\right)^{\dagger} (\boldsymbol{R} - \boldsymbol{\Psi}\boldsymbol{H}) = \left(\boldsymbol{D}\bar{\boldsymbol{H}}\right)^{\dagger} \boldsymbol{E} \tag{33}$$

where "†" denotes the pseudo-inverse and $\boldsymbol{E} \triangleq \boldsymbol{R} - \boldsymbol{\Psi}\boldsymbol{H}$ is the residual signal.

Therefore, based on MFDSM model, the off-grid DOA estimation by alternating descent iteration (MFDSM-OGDEADI) can be obtained and it can solve the optimal solution of (27). Then we can summarize the procedure flow of the MFDSM-OGDEADI algorithm in Tab. 1 below.

Through the above iterative algorithm, the sparse solution $\hat{\boldsymbol{H}}$ can be solved and then the spatial spectrum is constructed by

$$\boldsymbol{P}(\theta) = \left|\hat{\boldsymbol{H}}\right| / \max\left\{\left|\hat{\boldsymbol{H}}\right|\right\} \tag{34}$$

The peaks of spatial spectrum are searched to obtain the grid angles closest to the incident angles

$$\bar{\theta}_{l_k} = \arg\max_{\theta} \boldsymbol{P}(\theta) \tag{35}$$

then the angular deviation vector $\hat{\boldsymbol{\Gamma}}$ is corrected and the off-grid DOA estimation $\theta_k = \bar{\theta}_{l_k} + \Delta_{l_k}$ can be obtain.

V. SIMULATION RESULTS AND ANALYSIS

In this section, a lot of simulation experiments are performed to prove the performance improvement of our proposed MFDSM-OGDEADI algorithm compared to the state-of-the-art algorithms. In the simulation below, a standard ULA array with 8 sensors is adopted. The array sensor spacing is set as the half wavelength of the LFM signal's highest frequency. The grid size is set to 2° as a default.

A. SPATIAL SPECTRUM COMPARISON

Consider three wideband LFM signals and their energy distribution in the fractional domain is shown in Fig. 1. Fig. 1(a) and Fig. 1(b) are the case of incoherent and coherent LFM signals, respectively. The incident signal angles are the same in both cases, 81.215°, 75.372° and 109.581°, respectively. It can be seen that the three incoherent LFM signals are separable in the fractional domain, thus we can extract three peak-values of three LFM signals and then perform the DOA estimation for each peak-value separately, however, the three coherent LFM signals are inseparable in the fractional domain, thus we can only extract one peak-value and then perform the DOA estimation only once to estimate three signal angles.

Fig. 2 shows different DOA estimation algorithms' spatial spectrum (enlarged view) for the first LFM signal in

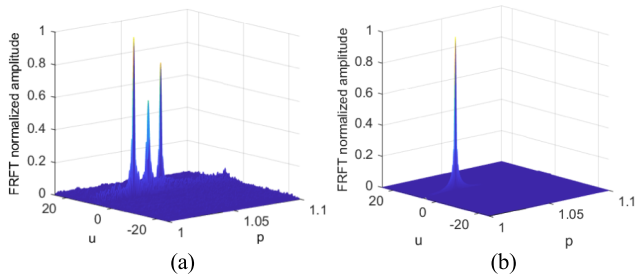

FIGURE 1. LFM signal energy distribution in the fractional domain. (a) Incoherent signal case. (b) Coherent signal case.

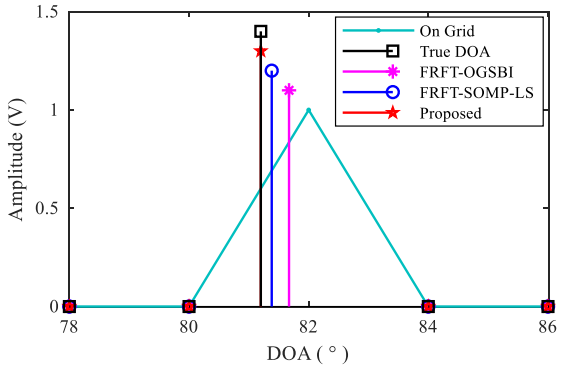

FIGURE 2. Spatial spectrum comparison (for the first LFM signal).

TABLE 2. Comparison of simulation results (unit: degree).

	Signal #1	Signal #2	Signal #3
True DOA	81.215	75.372	109.581
On Grid	82	76	110
FRFT-OGSBI	81.6783	75.8664	109.7497
FRFT-SOMP-LS	81.3937	75.6238	109.4856
MFDSM-OGDEADI	81.2474	75.3906	109.5662

incoherent signal case, where the sampling points is 2500 in time domain, whereas the snapshot is 1 in fractional domain. The SNR is set to 0dB. In the simulation, "On Grid" is obtained by the FRFT-BPDN algorithm with grid meshing, whereas the FRFT-BPDN, FRFT-OGSBI and FRFT-SOMP-LS algorithm are obtained by performing FRFT transform on the received data and then estimating DOAs using BPDN [32], OGSBI [21] and SOMP-LS [23] algorithm respectively.

For a better comparison, Table 2 gives the detailed estimation results of the different algorithms for the three incoherent LFM signals.

Seen from Fig. 2 and Table 2, when the grid size is large, the DOA estimation algorithm using On Grid has a large deviation from the true DOA angle, whereas the algorithms using grid mismatch (FRFT-OGSBI, FRFT-SOMP-LS and our proposed algorithm) can compensate the deviation appropriately. Under the same conditions, the compensation effect of the proposed algorithm is better. For incoherent wideband LFM signals, their DOA estimation is relatively easy, since they are almost separable in the fractional domain. However, it is more difficult for coherent wideband LFM signal's DOA estimation, because they are almost inseparable in the fractional domain, only single snapshot data can be used for DOA estimation, which results in a decrease in estimated performance. Therefore, the following discussion in the paper focuses on coherent wideband LFM signal's off-grid DOA estimation performance.

B. ANALYSIS IN TERMS OF SNR

This subsection intends to present a detailed performance analysis on the aforementioned algorithms to illustrate the superiority of our methods. The root mean square error (RMSE) is used for DOA estimation precision evaluation.

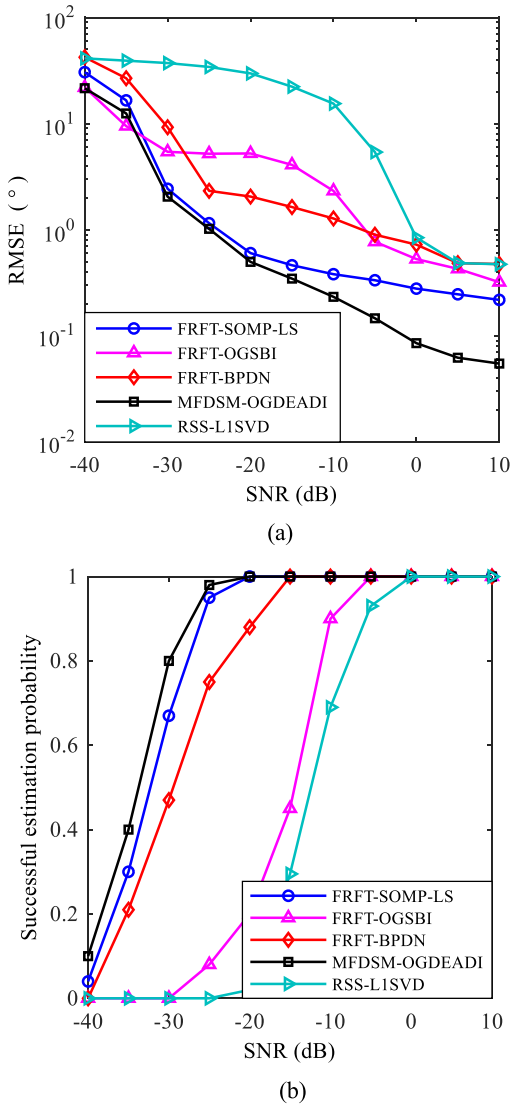

FIGURE 3. DOA estimation performances versus SNRs (in large angle difference condition). (a) Estimated RMSE. (b) Successful probability of estimation.

Fig. 3 and Fig. 4 show the relationship between DOA estimation performance and signal-to-noise ratio for different DOA estimation algorithms under large angle difference condition and small angle difference condition respectively.

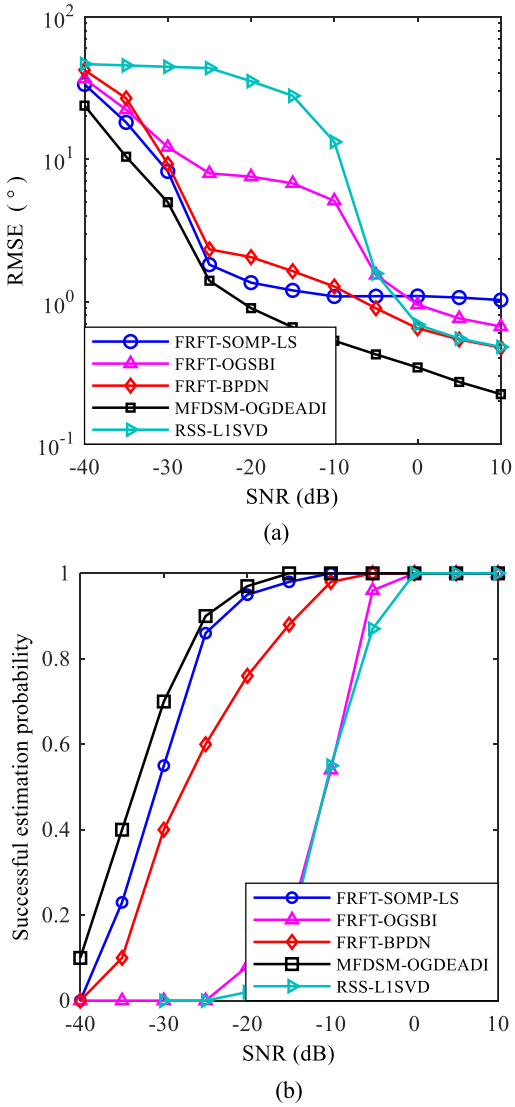

FIGURE 4. DOA estimation performances versus SNRs (in small angle difference condition). (a) Estimated RMSE. (b) Successful probability of estimation.

Fig. 3 is a case where the angle difference is larger than the array beamwidth (for $M = 8$, the beamwidth is 16.4°), whereas Fig. 4 is a case where the angle difference is smaller than the array beamwidth. In the simulation, the classic RSS-L1SVD [33] algorithm uses an ideal DOA pre-estimation.

As can be seen from Fig. 3 and Fig. 4, MFDSM-OGDEADI algorithm can provide the best estimation performance regardless of large or small angle difference. Among the algorithms, RSS-L1SVD and FRFT-BPDN are based on grid meshing, except that the former performs frequency domain DOA estimation and the latter performs fractional domain DOA estimation. Relatively speaking, FRFT-BPDN algorithm has better performance, but since the true DOA of the signal does not fall on the grid, its performance will not decrease as SNR increase when the SNR is greater than 5dB. For the other three algorithms based on grid mismatch (FRFT-OGSBI, FRFT-SOMP-LS and MFDSM-OGDEADI), the FRFT-OGSBI algorithm is sensitive to noise and results in poor performance at low SNR, while FRFT-SOMP-LS the algorithm adopts the simple OMP algorithm as the sparse recovery algorithm, and its estimation accuracy is not as good as the ReFOCUSS algorithm used in this paper. Therefore, the proposed algorithm can provide better estimation performance than the other two algorithms.

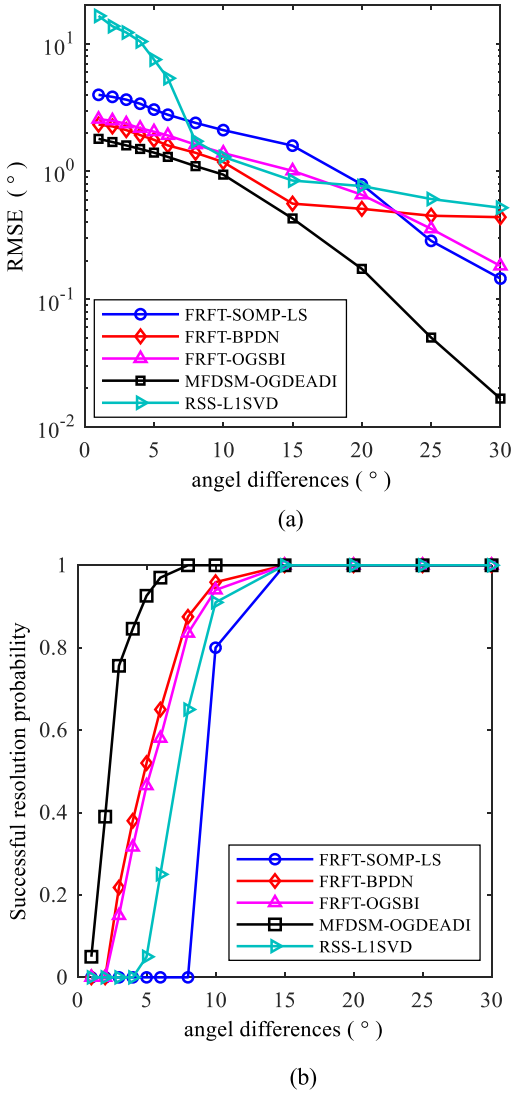

FIGURE 5. DOA estimation performances versus angel differences of signals. (a) Estimated RMSE. (b) Successful probability of estimation.

C. ANALYSIS IN TERMS OF ANGLE DIFFERENCE

We evaluate different DOA algorithms' angular resolution performance in this subsection. The statistical results for the coherent wideband LFM signals are shown in Fig. 5. Also, the relationship between DOA estimation error and successful resolution probability and the angle difference between signals in different coherent wideband LFM signals' estimation algorithms are demonstrated in Fig. 5. In the simulation, it is assumed that the DOA angle of the first signal is fixed

as θ_1 and the DOA angle of the second signal is set to $\theta_2 = \theta_1 + \Delta\theta$, where $\Delta\theta$ is the angular difference. In addition, the SNR is set to 0dB and the classic RSS-L1SVD algorithm still uses ideal DOA pre-estimation.

From Fig. 5, we can see that the estimation errors of all algorithms decrease as the angle difference increases. However, for the RSS-L1SVD and FRFT-BPDN algorithms based on meshing, due to the difference between the grid and the true angle, the estimation error will not drop sharply as angle difference increase after the angle difference is greater than a certain degree. For the other three algorithms based on mesh mismatch, the FRFT-SOMP-LS algorithm has poor angular resolution due to the OMP algorithm. The FRFT-OGSBI algorithm provides better performance than FRFT-SOMP-LS in terms of successful resolution probability when the angle difference is less than 20°. When the angle difference is larger than 20°, their resolution probability can reach 100%, whereas the estimation error of FRFT-OGSBI algorithm is slightly inferior to FRFT-SOMP-LS algorithm. The MFDSM-OGDEADI algorithm is superior to other algorithms in both estimation error and successful resolution probability.

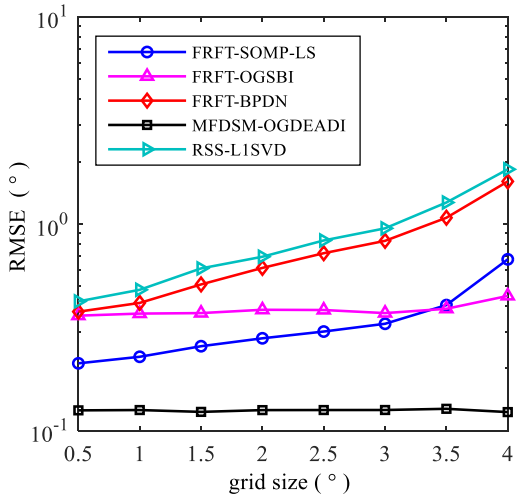

FIGURE 6. DOA estimation RMSE versus grid size.

D. ANALYSIS IN TERMS OF GRID SIZE

This subsection presents the DOA estimation performance under different grid size. In Fig. 6, the statistical results for the coherent wideband LFM signals are shown. In the simulation, it is the same as above that the coherent wideband LFM signal's basic setting, in which the two adjacent wideband signals from [78.651°, 122.384°] impinge onto the array simultaneously and the SNR is set to 0dB. In addition, RSS-L1SVD algorithm still uses the ideal DOA pre-estimation.

As can be seen from Fig. 6, the estimation errors of RSS-L1SVD and FRFT-BPDN algorithms increase with the increase of the grid size, since they are based on the grid meshing, the bigger grid sizes will bring the greater deviations from the true angles. The FRFT-SOMP-LS algorithms based on the grid mismatching compensates for this deviation and makes its estimation error smaller, but the increase in the grid size will still increase the estimation error. However, the FRFT-OGSBI and MFDSM-OGDEADI algorithms are basically unaffected by the grid size, but the MFDSM-OGDEADI algorithm is superior in terms of estimation error.

E. ANALYSIS IN TERMS OF THE ANGLE BIAS BETWEEN THE GRID AND THE TRUE ANGLE

This subsection presents the DOA estimation performance under different angular bias, as shown in Fig. 7. In the simulation, the SNR is set to 0 dB and the grid size is set to 2°. In addition, the RSS-L1SVD algorithm still uses the ideal DOA pre-estimation.

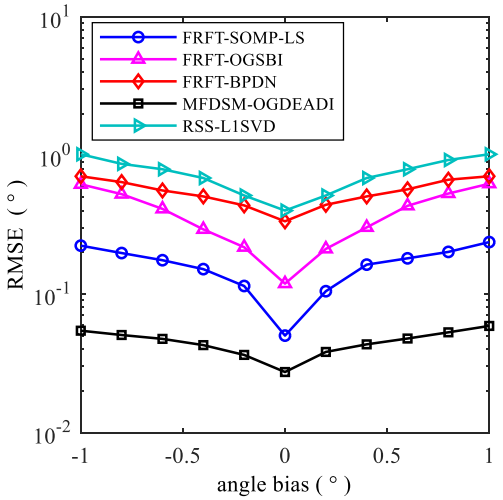

FIGURE 7. DOA estimation RMSE versus angle bias.

As can be seen in Fig. 7, the estimation errors basically exhibit a symmetric distribution centered on 0, that is, the estimation error is independent of the positive or negative angle bias, and is only related to its absolute value. At the same time, it can be seen that the sensitivity of different algorithms to angular bias is slightly different. For FRFT-OGSBI and FRFT-SOMP-LS algorithms, their estimation errors change faster as the angular bias increases, indicating that they are more sensitive to angular bias. Whereas for the other three algorithms, their estimation error is relatively flat with the increase of the angular bias, so the sensitivity is weak. However, from the perspective of estimated error, MFDSM-OGDEADI algorithm can provide better performance.

VI. CONCLUSIONS AND FUTURE WORKS

In this paper, the problem of wideband LFM signal's DOA estimation in the off-grid scenario has been studied, which is very common in reality. Making use of LFM signal's characteristics with high aggregation in the fractional domain, the conventional DOA estimation model is modified and a modified fractional domain sparse model is derived. Based on this model, a novel off-grid DOA estimation method using alternating descent iteration is proposed. And a large number of simulations are make and compared to existing classical

methods to verify the effectiveness of the proposed algorithm. The simulation results show that our proposed method can provide better estimation performance.

In the future works, we will further consider more general wideband signals for the problems of off-grid DOA estimation. In addition, the higher precision and more efficient algorithms will also be studied.

REFERENCES

[1] H. Krim and M. Viberg, "Two decades of array signal processing research: The parametric approach," *IEEE Signal Process. Mag.*, vol. 13, no. 4, pp. 67–94, Jul. 1996.
[2] W. Wang, Y. Jiang, and D. Wang, "Through wall human detection based on stacked denoising autoencoder algorithm," *J. Tianjin Normal Univ. (Natural Sci. Ed.)*, vol. 37, no. 5, pp. 50–54, 2017.
[3] Z. Liu, J. Chen, Y. Tong, F. Duan, and M. Ji, "Research and implementation of digital baseband signal transmission," *J. Tianjin Normal Univ. (Natural Sci. Ed.)*, vol. 38, no. 1, pp. 51–55, 2018.
[4] W. Li, Y. Zhan, J. Lin, R. Guo, and Z. Chen, "Wideband direction of arrival estimation in the presence of unknown mutual coupling," *Sensors*, vol. 17, no. 2, p. 230, Feb. 2017.
[5] S. Valaee and P. Kabal, "Wideband array processing using a two-sided correlation transformation," *IEEE Trans. Signal Process.*, vol. 43, no. 1, pp. 160–172, Jan. 1995.
[6] X. Liu *et al.*, "A multichannel cognitive radio system design and its performance optimization," *IEEE Access*, vol. 6, pp. 12327–12335, 2018.
[7] S. Mingzhu and G. Xianwei, "Parameters identification method via cepstrum analysis for mix blurred image restoration," *J. Tianjin Normal Univ. (Natural Sci. Ed.)*, vol. 37, no. 5, pp. 60–65, 2017.
[8] M. Wax, T.-J. Shan, and T. Kailath, "Spatio-temporal spectral analysis by eigenstructure methods," *IEEE Trans. Acoust., Speech, Signal Process.*, vol. 32, no. 4, pp. 817–827, Aug. 1984.
[9] H. Wang and M. Kaveh, "Coherent signal-subspace processing for the detection and estimation of angles of arrival of multiple wide-band sources," *IEEE Trans. Acoust., Speech, Signal Process.*, vol. 33, no. 4, pp. 823–831, Aug. 1985.
[10] D. Malioutov, M. Çetin, and A. S. Willsky, "A sparse signal reconstruction perspective for source localization with sensor arrays," *IEEE Trans. Signal Process.*, vol. 53, no. 8, pp. 3010–3022, Aug. 2005.
[11] M. M. Hyder and K. Mahata, "Direction-of-arrival estimation using a mixed $\ell_{2,0}$ norm approximation," *IEEE Trans. Signal Process.*, vol. 58, no. 9, pp. 4646–4655, Sep. 2010.
[12] D. Xu, N. Hu, Z. Ye, and M. Bao, "The estimate for DOAs of signals using sparse recovery method," in *Proc. IEEE Int. Conf. Acoust., Speech Signal Process. (ICASSP).*, vol. 22, no. 10, Mar. 2012, pp. 2573–2576.
[13] X. Liu, F. Li, and Z. Na, "Optimal resource allocation in simultaneous cooperative spectrum sensing and energy harvesting for multichannel cognitive radio," *IEEE Access*, vol. 5, pp. 3801–3812, 2017.
[14] Z.-M. Liu, Z.-T. Huang, and Y.-Y. Zhou, "An efficient maximum likelihood method for direction-of-arrival estimation via sparse Bayesian learning," *IEEE Trans. Wireless Commun.*, vol. 11, no. 10, pp. 1–11, Oct. 2012.
[15] S. Ma and Y. Wang, "Design and implementation of an ultra-wideband high-accuracy ranging system," *J. Tianjin Normal Univ. (Natural Sci. Ed.)*, vol. 37, no. 6, pp. 55–57, 2017.
[16] X. Wu, W.-P. Zhu, and J. Yan, "Direction of arrival estimation for off-grid signals based on sparse Bayesian learning," *IEEE Sensors J.*, vol. 16, no. 7, pp. 2004–2016, Apr. 2016.
[17] Q. Shen *et al.*, "Underdetermined wideband DOA estimation of off-grid sources employing the difference co-array concept," *Signal Process.*, vol. 130, no. 1, pp. 299–304, 2017.
[18] M. Chen, W. Wang, M. Barnard, and J. Chambers, "Wideband DoA estimation based on joint optimisation of array and spatial sparsity," in *Proc. 25th Eur. Signal Process. Conf. (EUSIPCO)*, Aug./Sep. 2017, pp. 2106–2110.
[19] Q. Liu, H. C. So, and Y. Gu, "Off-grid DOA estimation with nonconvex regularization via joint sparse representation," *Signal Process*, vol. 140, pp. 171–176, Nov. 2017.
[20] X. Liu, M. Jia, Z. Na, W. Lu, and F. Li, "Multi-modal cooperative spectrum sensing based on Dempster-Shafer fusion in 5G-based cognitive radio," *IEEE Access*, vol. 6, pp. 199–208, Oct. 2017.
[21] H. Zhu, G. Leus, and G. B. Giannakis, "Sparsity-cognizant total least-squares for perturbed compressive sampling," *IEEE Trans. Signal Process.*, vol. 59, no. 5, pp. 2002–2016, May 2011.
[22] Z. Yang, L. Xie, and C. Zhang, "Off-grid direction of arrival estimation using sparse Bayesian inference," *IEEE Trans. Signal Process.*, vol. 61, no. 1, pp. 38–43, Jan. 2013.
[23] A. Gretsistas and M. D. Plumbley, "An alternating descent algorithm for the off-grid DOA estimation problem with sparsity constraints," in *Proc. 20th Eur. Signal Process. Conf. (EUSIPCO)*, Aug. 2012, pp. 874–878.
[24] L. B. Almeida, "The fractional Fourier transform and time-frequency representations," *IEEE Trans. Signal Process.*, vol. 42, no. 11, pp. 3084–3091, Nov. 1994.
[25] E. Sejdić, I. Djurović, and L. Stanković, "Fractional Fourier transform as a signal processing tool: An overview of recent developments," *Signal Process.*, vol. 91, no. 6, pp. 1351–1369, Jun. 2011.
[26] W. Lu, Y. Gong, X. Liu, J. Wu, and H. Peng, "Collaborative energy and information transfer in green wireless sensor networks for smart cities," *IEEE Trans. Ind. Informat.*, vol. 14, no. 4, pp. 1585–1593, Apr. 2018.
[27] S. Chandran and M. K. Ibrahim, "DOA estimation of wide-band signals based on time-frequency analysis," *IEEE J. Ocean. Eng.*, vol. 24, no. 1, pp. 116–121, Jan. 1999.
[28] X. Liu, M. Jia, X. Zhang, and W. Lu, "A novel multi-channel Internet of Things based on dynamic spectrum sharing in 5G communication," *IEEE Internet Things J.*, to be published. doi: 10.1109/JIOT.2018.2847731.
[29] X. Zhang and Z. Zhang, "Near-field plate applied in wireless power transmission system," *J. Tianjin Normal Univ. (Natural Sci. Ed.)*, vol. 37, no. 6, pp. 58–61, 2017.
[30] Z. Hao, G. Leus, and G. B. Giannakis, "Sparse regularized total least squares for sensing applications," in *Proc. 11th Int. Workshop Signal Process. Adv. Wireless Commun. (SPAWC)*, Jun. 2010, pp. 1–5.
[31] I. F. Gorodnitsky and B. D. Rao, "Sparse signal reconstruction from limited data using FOCUSS: A re-weighted minimum norm algorithm," *IEEE Trans. Signal Process.*, vol. 45, no. 3, pp. 600–616, Mar. 1997.
[32] S. S. Chen, D. L. Donoho, and M. A. Saunders, "Atomic decomposition by basis pursuit," *SIAM J. Sci. Comput.*, vol. 20, no. 1, pp. 33–61, 1998.
[33] Y.-H. Zhao *et al.*, "A novel method of DOA estimation for wideband signals based on sparse representation," *J. Elect Inf. Techn.*, vol. 37, no. 12, pp. 2935–2940, Dec. 2015.

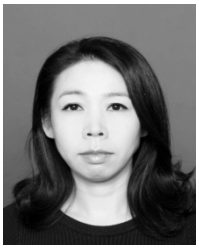

XIUHONG WANG received the bachelor's degree in communication engineering from Jilin University, China, in 2001, the master's degree in communication and information systems from Southeast University, China, in 2004, and the Ph.D. degree in information and communication engineering from the Harbin Institute of Technology, China, in 2017. From 2004 to 2006, she was with Trendchip Communication Technologies Co., Ltd., Suzhou, as an Algorithm Engineer. From 2006 to 2007, she was with the School of Information and Electrical Engineering, Harbin Institute of Technology, Weihai, China, as an Assistant Professor, where she has been a Lecturer, since 2007. Her research interests include array signal processing and direction-of-arrival estimation.

BO LI received the bachelor's degree in communication engineering, the master's degree, and the Ph.D. degree in information and communication engineering from the Harbin Institute of Technology, China, in 2007, 2009, and 2013, respectively. He was a Visiting Ph.D. Student with the School of Electrical and Electronic Engineering, Nanyang Technological University, Singapore, from 2012 to 2013. Since 2013, he has been with the School of Information and Electrical Engineering, Harbin Institute of Technology, Weihai, China, as a Lecturer. His research interests include physical-layer network coding, mobile ad hoc networks, and adaptive modulation and coding.

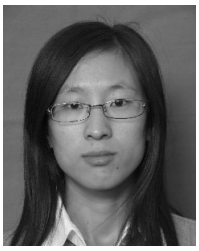

HONGJUAN YANG received the bachelor's degree in communication engineering from Jilin University, China, in 2007, the master's degree, and the Ph.D. degree in information and communication engineering from the Harbin Institute of Technology, China, in 2009 and 2013, respectively. She was a Visiting Ph.D. Student with the School of Electrical and Electronic Engineering, Nanyang Technological University, Singapore, from 2012 to 2013. Since 2013, she has been with the School of Information and Electrical Engineering, Harbin Institute of Technology, Weihai, China, as a Lecturer. Her research interests include cooperative diversity technology, physical-layer network coding, and delay-tolerant networks.

WEIDANG LU (S'08–M'13) received the Ph.D. degree in information and communication engineering from the Harbin Institute of Technology, in 2012. He was a Visiting Scholar with Nanyang Technology University, Singapore, The Chinese University of Hong Kong, and the Southern University of Science and Technology, China. He is currently an Associate Professor with the College of Information Engineering, Zhejiang University of Technology, Hangzhou, China. His current research interests include simultaneous wireless information and power transfer, wireless sensor networks, cooperative communications, and physical layer security for wireless systems.